Bifunctional Lewis and Brønsted acidic zeolites permit the continuous production of bio-renewable furanic ethers

D. Padovan,[a†] A. Al-Nayili[a†] and C. Hammond[a*]

The catalytic valorisation of bio-renewable feedstock often relies upon multi-stage processing of highly-functionalised substrates, resulting in selectivity and processs engineering challenges. Herein, we demonstrate that a bifunctional zeolitic material, containing both Lewis and Brønsted acid sites in a single catalytic material, permits the continuous production of bio-renewable furanic ethers, such as (butoxy)methyl furan, which possess potential as fuel additives. In contrast to mono-functional catalysts and physical mixtures thereof, the bifunctional Sn- and Al-containing BEA zeolite results in uniquely-high levels of activity, selectivity and stability. Optimal results were obtained over a bifunctional catalyst containing 2 wt.% Sn and 0.5 wt.% Al, prepared by modified solid state incorporation, which was highly selective (> 75 %) to the deisred ether for over 107 h on stream, and for over 3000 substrate turnovers.

Introduction

The depletion of fossil feedstock, coupled with the need for more environmentally sustainable chemical processing, drives the contemporary chemical community towards the sustainable utilisation of, preferably, renewable raw materials. The quest to employ such resources also relates to increasing population growth and to climate change. Lignocellulose, a complex mixture of lignin, cellulose and hemicellulose, is the most abundant bio-renewable feedstock inedible to humans. Consequently, the valorisation of lignocellulose, or derivatives thereof, represents a key target of contemporary research. Amongst several methods of lignocellulose valorisation, catalytic methods employing heterogeneous materials offer great potential.[1]

Unfortunately, the chemical nature of lignocellulose and its derivatives differs greatly from traditional petrochemical feedstock. Lignocellulose-derived feedstock is highly functionalised, typically highly oxygenated, and exhibits poor levels of volatility and thermal stability. Consequently, traditional catalytic methodologies are unsuitable for its valorisation.[2] Accordingly, the development of more sustainable chemical processes requires the co-development of new catalytic methods and materials.

An emerging approach undergoing an intensive period of research involves the liquid-phase valorisation of so-called platform molecules, obtained through controlled depolymerisation and separation of lignocellulose and its key building blocks through *e.g.* hydrolysis.[3] Amongst such feedstock, the catalytic valorisation of C_5- and C_6-based furanics, such as 5-hydroxymethyl furfural (HMF) and furfural (FF), has received widespread attention.[4] Indeed, the catalytic conversion of furfural can produce a variety of useful products, and furfuryl alcohol and its ethers are intermediates for the synthesis of γ-valerolactone (GVL), and its ethers also possess particular promise as fuel additives.[5] Although a wide range of materials, conditions and approaches have been explored for furfural valorisation, few works have truly demonstrated high levels of selectivity and stability. In fact, obtaining high selectivity to a single product is a major challenge during all biomass-to-chemicals research, given the highly functionalised nature of the reactive substrates. Although terms such as "useful product selectivity" are now routinely employed, the cost of separation in catalytic processes is sufficient that high selectivity to a single product must be attained. Moreover, catalyst stability under rigorous, continuous conditions also requires significant attention.

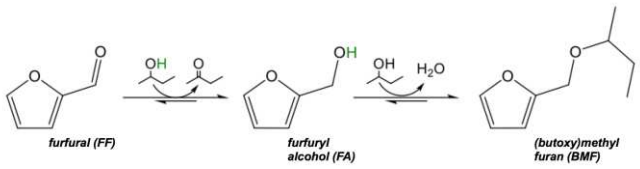

Scheme 1 Catalytic formation of furanic ethers from furfural.

Ethers of furfural and its derivatives (Scheme 1) hold particular promise as fuel additives.[5a] Whilst ethers are typically obtained through Brønsted acid catalysis, recent studies have indicated that Lewis acid-only systems may show good levels of activity and selectivity for such processes, with Lewis acidic silicates, such as Sn- and Hf-containing zeolite Beta, showing significant potential.[6] However, little is known about how Lewis acids catalyse such reactions, or what role adventitious Brønsted acidity possible exhibits. Moreover, although catalyst stability has been probed, high selectivity to ethers of furfural and 5-HMF has only been observed at relatively low turnover

[a.] *Cardiff Catalysis Institute, Cardiff University School of Chemistry, Main Building, Park Place, Cardiff, CF10 3AT, UK.*
† These authors contributed equally to this work.

numbers (< 250 turnovers), and the intermediate alcohol species are typically observed as major products after a particular period of operation.[6c] Given their notorious ability to polymerise and subsequently deactivate heterogeneous catalysts, the generation of such alcohols at high selectivity is far from desirable. Moreover, up to 35 % loss in conversion over the same number of turnovers was also observed in previous studies.[6c] Motivated by these observations, the major target of this work is to develop a catalytic system capable of selectively producing furanic ethers at high levels of selectivity, activity and stability.

Results and Discussion

Lewis-only systems. As described above, Lewis acidic silicates have previously demonstrated promising levels of activity, selectivity and stability for a range of biomass valorisation reactions, including transfer hydrogenation and etherification.[7] Accordingly, we focused upon the tandem transfer hydrogenation and etherification of furfural, a platform molecule obtained through the isomerisation and dehydration of xylose. Under conditions adapted from the transfer hydrogenation of various carbonyl compounds,[8] where 2-butanol is employed as H-donor, we first evaluated the catalytic performance of two stannosilicates containing different amounts of Sn^{IV} (2 and 10 wt. %) in batch reactors.[9] Both materials were prepared by solid-state incorporation, a two-step methodology requiring dealumination of an alumionsilicate precursor, followed by remetallation of the material with Sn^{IV}.[9,10] Metal contents, porosity data and XRD patterns of these materials are included in the supplementary information (ESI Figure S1, Table S1).

Under identical reaction conditions, including substrate/metal ratio (FF/Sn = 100), it is clear that 2Sn-β and 10Sn-β are both active for the transfer hydrogenation/etherification reaction, with up to 70 % conversion being obtained in 90 minutes (Figure 1, Left). In good agreement to our recent studies, 2Sn-β is approximately 30 % more active on a TOF basis (234 vs. 173 h^{-1}), indicating that 10Sn-β possesses a greater number of inactive Sn sites, as recently described in depth.[9] Despite their comparable activity, tremendous differences in selectivity are observed between both catalytic materials (Figure 1, Right). Whilst FA is the major reaction product obtained over 10Sn-β at all levels of conversion, 2Sn-β exhibits substantially higher selectivity to BMF at all levels of conversion. Although both catalysts exhibit slightly different levels of Lewis activity in terms of rate of FF conversion, the differences in intrinsic activity are not sufficient to solely explain the improved levels of selectivity, particular at all levels of conversion. Since 2Sn-β contains a greater fraction of silanol nests, present from the dealumination of the parent alumionsilicate as indicated by FTIR analysis (ESI Figure S2), [11] we hypothesise that contribution from these Brønsted sites may aid the etherification process to some extent.[12]

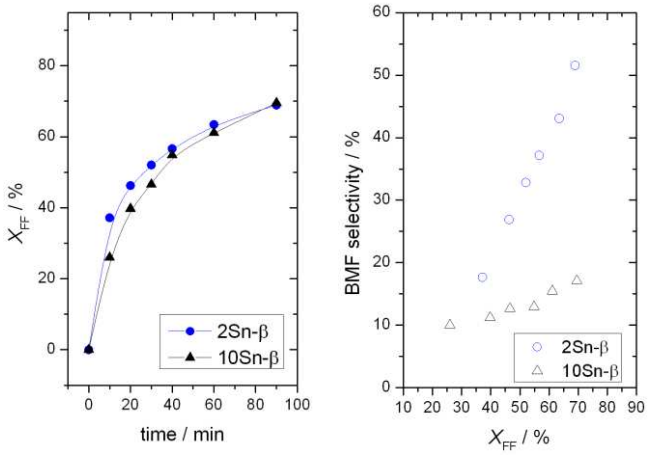

Figure 1 (Left) Rate of FF conversion over Sn-containing β zeolites, and (Right) selectivity to BMF as a function of FF conversion.

Having obtained the intrinsic kinetic and selectivity data, we subsequently set about exploring the activity and stability of 2- and 10-Sn-β in continuous flow reactors.[13] Continuous Plug Flow Reactors (PFR) offer major advantages over slurry reactors, including 1) improved safety and process control,[14] 2) higher levels of mass- and heat-transfer, 3) improved rates of reaction, 4) smaller reactor volumes, and 5) scalability. In addition, by operating under steady state conditions they allow detailed evaluation of catalyst stability.[15] The performance of these catalysts, and all further catalysts tested in continuous mode (*Vide Infra*), are compared in terms of activity (TOF, Equation 1), stability (Relative performance, Equation 2) and selectivity (S_{BMF}, Equation 3), all as a function of number of substrate turnovers (ρ, Equation 4). Comparing activity as a function of TON as opposed to time on stream allows true comparison of catalysts of disparate activity in terms of the amount of product produced.[15a] We note here that the contact time (τ, Equation 5) in the first two reactions was adjusted so that both catalysts exhibited a similar level of substrate conversion, in order to probe similar parts of the reaction coordinate, which is particularly important when comparing BMF selectivity.

$$\text{TOF} = \text{moles}_{(\text{FF converted})}\ \text{moles}^{-1}_{(\text{Sn})}\ \text{min}^{-1} \quad (1)$$

$$\text{Relative performance} = \frac{TOF_{(t)}}{TOF_{(0)}} \quad (2)$$

$$S_{(BMF)} = \frac{[BMF\}}{([FF]_0 - [FF]_t)} \times 100 \quad (3)$$

$$p = \frac{n(FF) per\ \min x\ \Sigma_t}{n(Sn)} \quad (4)$$

$$\text{Contact time} = \tau\ (min^{-1}) = \frac{volume_{(catalyst\ bed)}}{flow\ rate} \quad (5)$$

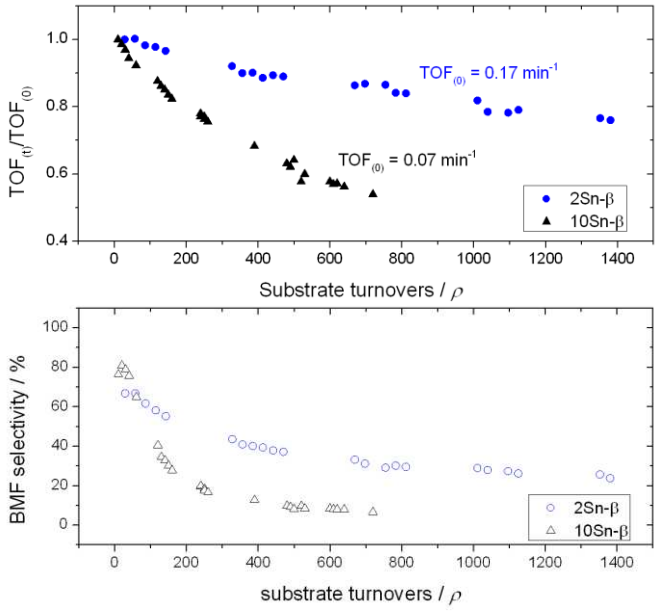

Figure 2 (Top) Relative performance and (Bottom) BMF selectivity displayed by 2- and 10-Sn-β, as a function of substrate turnover.

2- and 10-Sn-β exhibit substantial differences in performance in the continuous regime (Figure 2). Firstly, 2Sn-β is substantially more active under comparable conditions, with its TOF being approximately 2.5 times larger than that observed for 10Sn-β. In addition, 2Sn-β is also substantially more stable, with less than 20 % loss in performance observed over 1000 turnovers, equivalent to 10 batch reactions under typical literature conditions.[6] In contrast, 10Sn-β loses almost 50 % of its original activity after 700 turnovers.

In addition to higher degrees of activity and stability, 2Sn-β is also more selective to BMF than 10Sn-β, particularly at extended periods of operation. However, whilst 2Sn-β is more selective than 10Sn-β, neither catalyst exhibits high selectivity to BMF at an extended period of operation. Indeed, after approximately 300 turnovers, FA becomes the major reaction product for 2Sn-β, and the decrease in selectivity as a function of TON is even more dramatic for 10Sn-β, where BMF selectivity rapidly diminishes to < 20 %. We note here that in both cases, the selectivity balance is fully accounted for by FA and BMF. Accordingly, deactivation of the etherification process occurs more rapidly than for the TH process (Scheme 1). Thus, even if Lewis acid sites alone are capable of catalysing the two-step process, they are not able to do so with sufficient levels of activity and stability to be particularly interesting for continuous operation.

Catalytic etherification. To develop a selective and stable catalytic system, catalytic studies of the etherification reaction alone were performed, where FA was employed as substrate. In good agreement with the initial results, 2Sn-β is clearly more active for etherification than 10Sn-β, reaching a maximum conversion of 50 % in 90 minutes. To evaluate the potential role of silanol nests, dealuminated zeolite β was also evaluated. Despite exhibiting lower levels of activity than the Sn-containing analogues, the contribution of this activity can readily explain the differences in selectivity of 2- and 10-Sn-β, strongly indicating that a combination of Lewis and Brønsted acid sites may be a more effective catalytic system.

A variety of Brønsted acidic zeolites and mineral acids were thus screened (Figure 3), with a FA/H^+ ratio of 100 employed. Clearly, such catalysts are far more suitable for etherification catalysis, with H-β (SiO_2/Al_2O_3 = 300, henceforth H-β (300)) exhibiting the best levels of activity under the initial reaction conditions. Indeed, the activity of this catalyst was so high that mass transfer limitations were found to influence the rate of reaction at a FA/H^+ ratio of 100. Decreasing the amount of catalyst to reach the true kinetic regime (ESI Figure S3) revealed the initial activity of H-β (300) to be 4009 h^{-1}, in contrast to 119 h^{-1} for 2Sn-β alone. Accordingly, it is evident that a combination of Lewis and Brønsted acidity offers the best opportunity of achieving high yields and selectivity to BMF. Amongst mineral acids, H_2SO_4 was found to be the most active. However, the selectivity to BMF was much lower in this case than when the reaction was catalysed by H-β; whilst H-β always exhibits a BMF selectivity of > 80 %, reactions catalysed by H_2SO_4 resulted in high selectivity to butyl levulinate (ESI Figure S4).

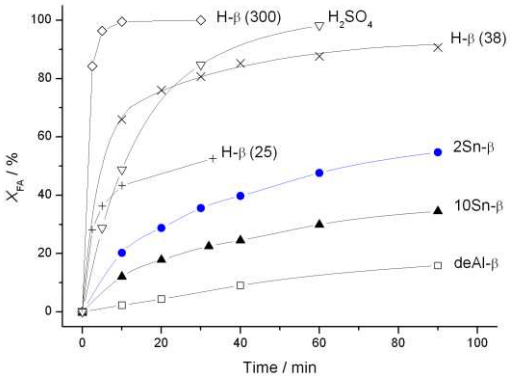

Figure 3 Rate of FA conversion as a function of time over a variety of Brønsted and Lewis acid catalysts.

Bifunctional catalytic systems. In order to obtain both Lewis and Brønsted acid capability, we first explored a hybrid catalytic system, comprising of a solid Lewis acid (2Sn-β) and a continuous feed of mineral acid (H_2SO_4). Such a hybrid approach, where Sn-β is employed in combination with a mineral acid, has previously shown to be effective for the production of 5-HMF from glucose, a two-step reaction that proceeds *via* Lewis-catalysed isomerisation and Brønsted-catalysed dehydration.[16] Unfortunately, this results primarily in the formation of butyl levulinate, and was not studied further.

Given the efficacy and selectivity of H-β (300) for the etherification reaction, we instead focused upon developing bifunctional, heterogeneous catalytic systems based on β zeolite. Two approaches were considered, including (1) the utilisation of simple physical mixtures of 2Sn-β and H-β (300), and (2) the preparation of a bifunctional Sn- and Al-containing β zeolite, in a similar manner to Dijkmans *et al.*[17] Such bifunctional materials, where both active components are hosted in one matrix, have shown unanticipated advantages for

some multi-step catalytic transformations, particularly where equilibrium or internal diffusion plays a role.[18]

The following section first describes optimisation of the physical mixture composition, prior to describing the synthesis and characterisation of bifunctional Sn- and Al-containing β zeolite.

Optimisation of physical mixture. Physical mixtures of solid Lewis and solid Brønsted acids have previously been employed for multi-step catalytic processes, such as the conversion of glucose to 5-HMF, and the and conversion of furfural to γ-valerolactone.[19] Based on the etherification results, a combination of 2Sn-β and H-β (300) was chosen. We first explored the potential of the physical mixture in batch reactors, in order to optimise the ratio of Lewis/Brønsted acidity. Unfortunately, the catalytic activity of 2Sn-β in terms of TH capability is somewhat compromised by the co-presence of H-β (300), given that the rate of FF conversion decreases slightly (Figure 4, Left). Notably, the decrease in rate correlates to the increase in H-β (300) loading. However, dramatic improvements in the selectivity of the reaction are observed, with BMF observed as the major reaction product in the presence of H-β (300) (Figure 4, Right). Optimal selectivity trends were observed at a H-β (300) mass charge of 30 mg, which resulted in 77 % selectivity to BMF at a FF conversion of ± 65 %. When greater amounts of H-β (300) were employed, a decrease in BMF selectivity was also observed, due to undesired ring opening. Given the decrease in TH rate and the increase in BMF ring opening at increasing H-β (300) masses, the optimal mass ratio of 2Sn-β to H-β is 4:1.

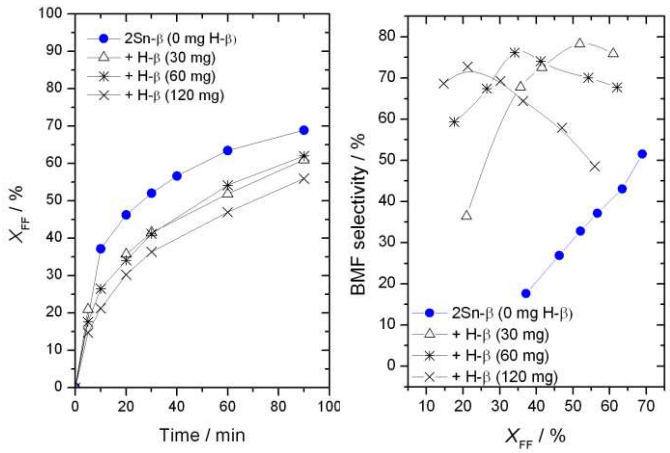

Figure 4 (Left) Rate of FF conversion and (Right) BMF selectivity as a function of FF conversion, over 2Sn-β in the co-presence of H-β (300).

Preparation and characterisation of bifunctional [Sn,Al]-β. As described above, solid state stannation requires dealumination of a parent aluminosilicate material, prior to the solid state incorporation of Sn^{IV} with Sn(II)acetate (Scheme 2).[10] By only partially dealuminating the zeolite, one can theoretically prepare a material containing both Lewis acidity from Sn^{IV}, and Brønsted acidity from residual Al^{III} in the zeolite framework. Such an approach was elegantly employed by Dijkmans *et al.* in order to prepare a bifunctional Sn- and Al-containing β zeolite.[17] In that case, the bifunctional catalyst was employed for the catalytic conversion of dihydroxyacetone to ethyl lactate in batch reactors, and Sn^{IV} was incorporated through grafting of $SnCl_4.5H_2O$ in dry isopropanol.

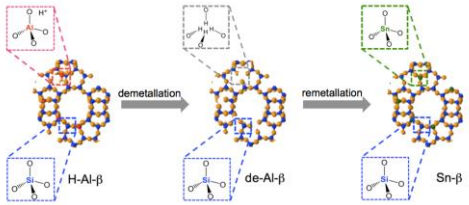

Scheme 2 Schematic of solid state incorporation.

Following the approach of Dijkmans *et al.,* partial dealumination of H-β (38) was achieved by treatment in 13 M HNO_3 for various periods of time. Amongst a range of times, treatment of H-β (38) for 1 h resulted in a material containing 0.16 wt. % Al as determined by ICP-MS. In agreement with our full dealumination studies, the crystalline structure of the β zeolite was unaffected by this treatment (ESI Figure S5). Given the poor sensitivity of DRIFTS studies with pyridine as a probe molecule, and the very low Al^{III} content, verification of the presence of Brønsted acid sites was obtained by ^{27}Al MAS NMR. This clearly demonstrated that the residual Al^{III} content was present within the zeolite framework, hence giving rise to Brønsted acid sites (Figure 5, Left).

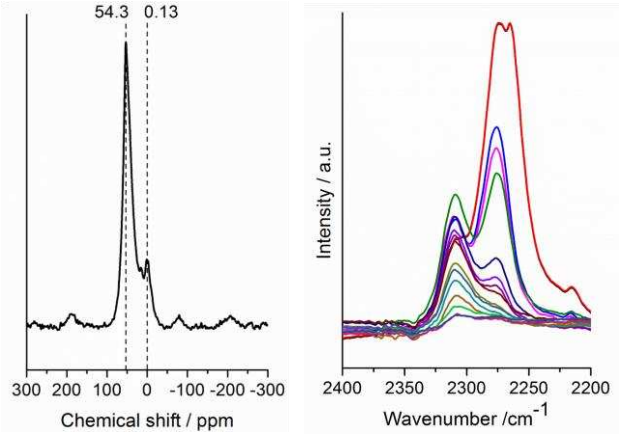

Figure 5 (Left) ^{27}Al MAS NMR spectrum of [2Sn, 0.16Al]-β and (Right) DRIFT studies with d_3-CD_3CN.

Subsequently, Sn^{IV} was incorporated into the partially dealuminated framework at a loading of 2 wt. %, consistent with the optimal loading from our initial studies. Verification of the Lewis acidic nature of the Sn^{IV} content was achieved by DRIFTS studies with d_3-CD_3CN as probe molecule, where the characteristic stretch 2309 cm^{-1} was present (Figure 5, Right).[20] No asymmetry, potentially indicative of open- or closed- Sn^{IV} sites was observed even following desorption at 200 °C. Accordingly, Lewis acidity is present from Sn (2 wt. %) and Brønsted acidity present from residual Al^{III} (± 0.16 wt.%). The catalyst is henceforth described as [2Sn,0.16Al]-β.

Continuous performance of physical mixtures and bifunctional catalysts. 2Sn-β/H-β (300) and [2Sn,0.16Al]-β were subsequently evaluated as bifunctional catalytic systems for the combined TH/etherification of furfural to BMF, and compared to the reference sample of purely Lewis acidic 2Sn-β. The contact time in each case was adjusted so that a similar stage of the reaction coordinate, in terms of FF conversion, was probed.

As can be seen (Figure 6), each catalytic system is relatively stable in terms of TH capability, with the relative performance decreasing by 10 - 30 % over approximately 600 substrate turnovers. However, bifunctional [2Sn,0.16Al]-β appears to exhibit slightly higher levels of deactivation, indicating it to be a poorer Lewis acid catalyst. Further indication of this is observed from the initial activity of each catalytic system. Indeed, whilst the initial rate of conversion over 2Sn-β and 2Sn-β/H-β are 0.17 and 0.19 min^{-1}, respectively, the rate observed over [2Sn,0.16Al]-β was only 0.08 min^{-1}, close to that of 10Sn-β, Figure 2, which is a material known to contain inactive, extra-framework SnOx species.[9]

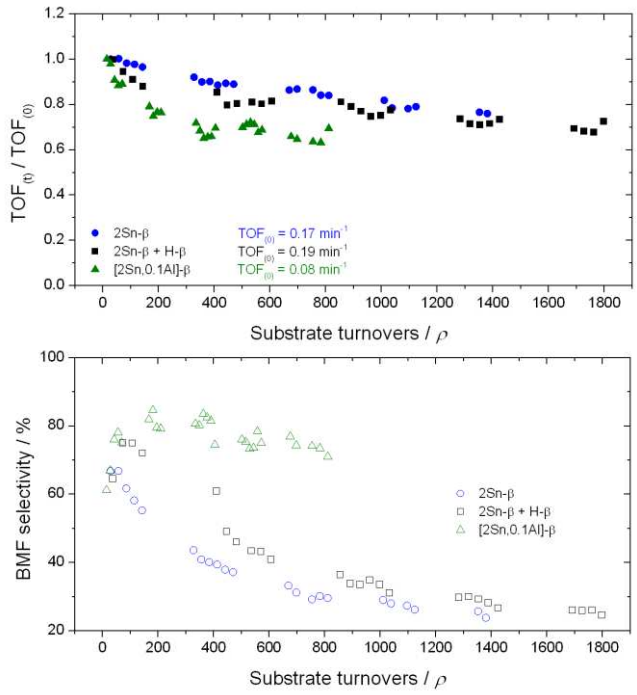

Figure 6 (Top) Relative performance and (Bottom) BMF selectivity displayed by 2-Sn-β, 2-Sn-β/H-β and [2Sn,0.16Al]-β, as a function of substrate turnover.

Despite slightly poorer performance in terms of TH catalysis, dramatic improvements in ether selectivity are obtained for the bifunctional solid catalyst. Indeed, after approximately 700 substrate turnovers, BMF selectivity is still close to 75 %. In contrast, the BMF selectivity observed over 2Sn-β and 2Sn-β/H-β at the same number of substrate turnovers is dramatically lower (± 30 %). Clearly, hosting both Lewis and Brønsted acidic active sites in the same matrix results in substantial improvements in BMF selectivity.

To account for the significant improvement in etherification stability, a variety of characterisation studies, such as TGA and porosimetry, were performed on the *ex reactor* samples of 2Sn-β/H-β and [2Sn,0.16Al]-β. However, no major differences in the used catalytic materials were observed (ESI Figure S6). Whilst etherification activity is lost for the physical mixture of 2Sn-β/H-β, the selectivity to FA compensates for the loss of selectivity *i.e.* the potential formation of an undesirable by-product does not occur. Accordingly, no clear differences between the used bifunctional catalytic beds can be observed, despite the vast differences in etherification activity after extended operation.

Given the known sensitivity of FA to polymerise and form undesirable by-products, leading to the deactivation of heterogeneous catalysts,[21] we hypothesise that hosting both Sn and Al in the same framework may lead to more facile conversion of FA to BMF than found over the physical mixture, where diffusion of FA out of the crystallites of 2Sn-β, and subsequently into the crystallites of H-β, needs to occur. Accordingly, deactivation may be related to the decreased steady state concentration of FA throughout the reaction period, by having close proximity of the Lewis and Brønsted acid sites of the catalyst.

Bifunctional [Sn,Al]-β prepared by solid state incorporation. To understand why [2Sn,0.16Al]-β exhibits poorer levels of Lewis acid activity than the fully dealuminated analogues, ^{119}Sn MAS NMR measurements were performed. As can be seen, at the same Sn loading *i.e.* 2 wt. %, a larger amount of extra-framework SnOx species (δ = -602 ppm) are observed in [2Sn,0.16Al]-β than in fully dealuminated 2Sn-β (note that isomorphously-substituted Sn^{IV} sites in their hydrated form are characterised by a resonance at -690 ppm). In fact, it is evident that a greater amount of inactive SnOx species is observed when there is a greater amount of residual Al^{III} in the framework (Figure 7). Unfortunately, this clearly indicates that incorporating Sn^{IV} into a partially dealuminated framework by solid state incorporation is hindered by the co-presence of residual Brønsted acid sites.

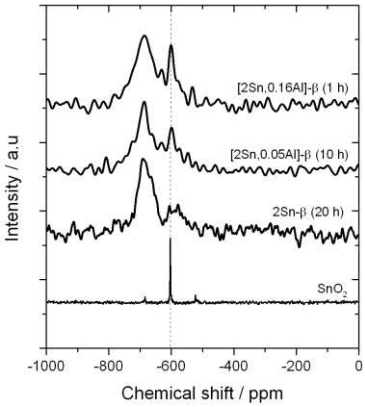

Figure 7 ^{119}Sn MAS NMR spectra of bifunctional samples of Sn and Al-containing β zeolites. Each sample contains 2 wt. % Sn, and the time of dealumination for each sample is added in parenthesis.

To overcome this, we explored an alternative synthesis strategy, involving the incorporation of both Sn^{IV} *and* Al^{III} into a fully dealuminated zeolite framework.[22] Accordingly, the solid state incorporation method was modified so that a suitable Al precursor (in this case Al(III)acetyl acetonate) was present along side Sn(II)acetate during the preparation process.[23] A material

with a Sn loading of 2 wt. %, and an Al^{III} loading of 0.5 wt. % was subsequently prepared, and is denoted as [2Sn,0.5Al]-β.

To verify that Al^{III} was reincorporated into the framework, and hence verify the presence of both Lewis and Brønsted acid sites in [2Sn,0.5Al]-β, ^{27}Al MAS NMR was performed. As can be seen (ESI Figure S7), Al^{III} is almost exclusively present as tetrahedral Al^{III}, characteristic of isomorphously substituted Al^{III}. DRIFTS studies with pyridine as probe molecule were also performed, in order to verify the bifunctionality of the material.[24] Despite the low Al^{III} loading of [2Sn,0.5Al]-β, the presence of both Lewis and Brønsted acid sites in all the spectra (even those heated to 200 °C) is evident (Figure 8). Absorption bands at 1643 and 1540 cm^{-1} correspond to Brønsted sites, whilst those at 1595 and 1450 cm^{-1} correspond to the interaction between pyridine and Lewis acid sites. Accordingly, it is clear that a bifunctional catalyst consisting of both Lewis and Brønsted acidity has been prepared by modified solid state incorporation.

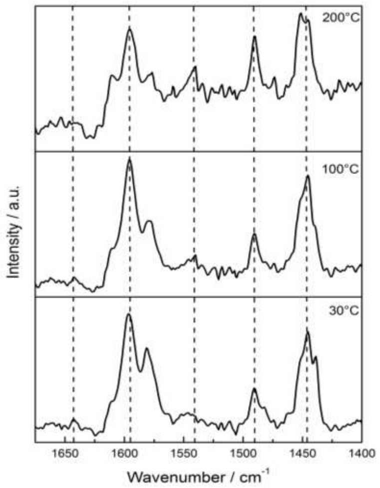

Figure 8 DRIFT studies of [2Sn,0.5Al]-β, with pyridine as probe molecule.

The catalytic properties of [2Sn,0.5Al]-β were subsequently evaluated in the continuous regime (Figure 9). In contrast to [2Sn,0.16Al]-β, which exhibited lower rates of conversion due to the presence of extra-framework SnOx species, the initial activity of [2Sn,0.5Al]-β is no lower than that exhibited by Lewis acidic 2Sn-β[illegible]°[illegible]. This indicates that the Lewis acidity of these materials is comparable. Moreover, the BMF selectivity obtained over [2Sn,0.5Al]-β is also comparable to [2Sn,0.16Al]-β, and substantially higher at a given number of turnovers than 2Sn-β. This indicates that the realumination strategy is more suitable for the introduction of Brønsted acidity than the partial dealumination approach. These observations confirm that modified solid state incorporation is a more suitable method of preparing bifunctional Lewis and Brønsted acidic Sn,Al-β than the partial dealumination approach.

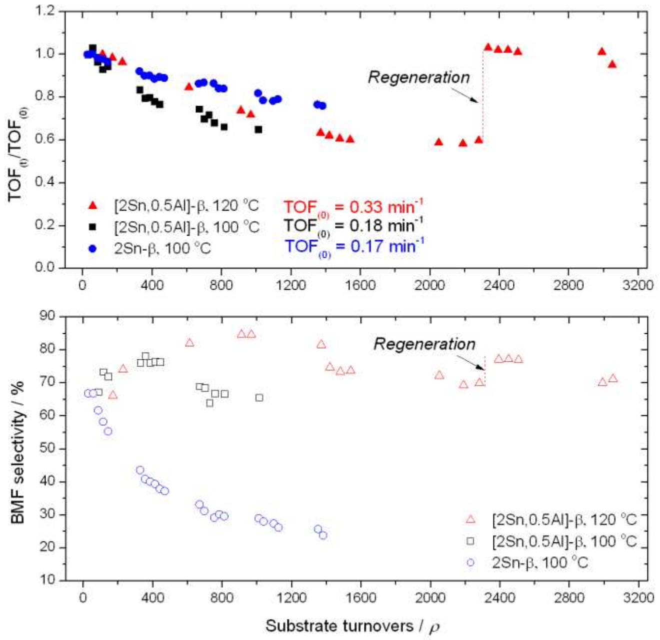

Figure 9 (Top) Relative performance and (Bottom) BMF selectivity displayed by 2Sn-β and [2Sn,0.5Al]-β at 100 and 120 °C as a function of substrate turnover.

The reaction conditions in the presence of the optimal bifunctional catalyst, [2Sn,0.5Al]-β, were subsequently optimised. Operating the reactor at elevated temperatures (120 °C) was found to increase both the productivity (initial TOF of 0.33 min^{-1}), and the BMF selectivity, which was held above 70 % even after > 2000 substrate turnovers (corresponding to 80 h on stream) during an initial operational cycle. In addition to long term BMF selectivity, the initial activity (0.33 mol converted min^{-1}) and number of turnovers achieved by the optimised catalytic system (2300 during the initial period) are an order of magnitude higher than previously reported in the literature for similar reactions.[6c]

To investigate the potential mechanisms of deactivation, *ex reactor* characterisation of the used catalytic materials was performed. This revealed that the long-range order of all the catalytic materials was maintained even after extended operation (ESI Figure S8), but that loss in porosity occurred (ESI Table S2). In fact, after 2300 turnovers the surface area and micropore volume of [2Sn,0.5Al]-β decreased by 43 % and 49 %, respectively (ESI Table S2). Notably, the loss in porosity correlates very closely to the loss in performance (< 40 %) over the initial period. This strongly indicates that fouling of the micropores occurs during extended operation. Given that fouling is typically non-permanent, we investigated the potential suitability of regeneration protocols. Full performance of the system – in terms of activity *i.e.* conversion, and BMF selectivity, could be restored following simple heat treatment of the catalyst in air at 550 °C. Accordingly, over 3000 substrate turnovers (107 h time on stream) at a BMF selectivity > 70 % could be achieved with only one regeneration procedure being employed.

Conclusions

The catalytic conversion of furfural to (butoxymethyl) furan was studied in the batch and continuous regime. Optimisation of a bifunctional zeolite material, possessing both Brønsted and Lewis acid sites from Al^{III} and Sn^{IV}, resulted in a catalytic system more selective, active and stable than monofunctional analogues or physical mixtures thereof. A maximum BMF selectivity of 87 % was obtained for a catalyst consisting of 2 wt. % Sn and 0.5 wt. % Al, which was prepared by modified solid state incorporation of a dealuminated β zeolite precursor, and which operated at 120 °C. Continuous operation for over 3000 turnovers (107 h on stream) was achieved. The high activity, selectivity and durability of this catalytic material are over an order of magnitude higher than observed in comparable systems, and demonstrates that high selectivity to a single product can be obtained during biomass upgrading, despite the highly functionalised nature of the substrate and its products.

Experimental

Catalyst synthesis

Commercial zeolite Al-β (Zeolyst, NH_4-form) was dealuminated by treatment in HNO_3 solution (13 M HNO_3, 100 °C, 20 mL g^{-1} zeolite, 20 hours if not specified differently in the text). Solid-state stannation of dealuminated zeolite β was performed the procedure reported in reference 8, by grinding the appropriate amount of tin (II) acetate with the necessary amount of dealuminated zeolite for 10 minutes in a pestle and mortar. Following this procedure, the sample was heated in a combustion furnace (Carbolite MTF12/38/400) to 550 °C (10 °C min^{-1} ramp rate) first in a flow of N_2 (3 h) and subsequently air (3 h) for a total of 6 h. Gas flow rates of 60 mL min^{-1} were employed at all times. Bifunctional Al/Sn-Beta was made by solid state incorporation of tin (II) acetate and aluminium (III) acetylacetonate pentahydrate into a dealuminated zeolite Beta following the same procedure described above. Proton form from the NH_4-form of the Al-Beta zeolites (H-β) were obtained after a treatment at 550°C in a tubular furnace for 3h under air flow.

Catalyst characterisation

A PANalytical X'PertPRO X-ray diffractometer was employed for powder XRD analysis. A CuKα radiation source (40 kV and 30 mA) was utilised. Diffraction patterns were recorded between 6-55° 2θ (step size 0.0167°, time/step = 150 s, total time = 1 h). Specific surface area was determined from nitrogen adsorption using the BET equation, and microporous volume was determined from nitrogen adsorption isotherms using the t-plot method. Porosymetry measurements were performed on a Quantachrome Quadrasorb, and samples were degassed prior to use (105°C, 6h, nitrogen flow). Adsorption isotherms were obtained at 77 K. TGA analysis was performed on a Perkin Elmer system. Samples were held isothermally at 30 °C for 30 minutes, before being heated to 550 °C (10 °C min^{-1} ramp rate) in air. MAS NMR experiments were performed at Durham University through the EPSRC UK National Solid-state NMR Service. Samples were measured under conditions identical to those reported by Bermejo-Deval *et al.,*[25] and Hammond and co-workers.[26]

DRIFT spectroscopy was performed in a Harrick praying mantis cell. The spectra were recorded on a Bruker Tensor spectrometer over a range of 4000-650 cm-1 at a resolution of 2 cm-1. *In situ* CD_3CN and Pyridine measurements were performed on pre-treated zeolite powders (550 °C, 1 hour under flowing air, 60 mL min-1) as follows: following pre-treatment, the sample was dosed with the probe molecule vapour at room temperature for 5 minutes, and one spectrum was recorded. The sample chamber was subsequently evacuated under dynamic vacuum (approximately 10^{-4} mbar), and spectra were recorded at 30, 100 and 200 °C.

Kinetic evaluation and analytical methods

Batch TH and etherification reactions with furfural (or furfuryl alcohol) were performed in a 100 mL round bottom flask equipped with a reflux condenser, which was thermostatically controlled by immersion in a silicon oil bath. The vessel was charged with a 10 mL solution of FF (or FA) in 2-butanol (0.2M), which also contained an internal standard (biphenyl, 0.01M). The solution was subsequently heated to the desired temperature (98 °C internal temperature). The reaction was initiated by addition of an appropriate amount of catalyst, typically corresponding to 1 mol. % Sn (or Al) relative to the reactant. The solution was stirred at ± 800 rpm with an oval magnetic stirrer bar.

Batch homogeneous etherification reactions were conducted in a similar experimental setup, the reaction was started by adding a precise volume of concentrated aqueous solution of the mineral acid into the reactant solution in order to have a 10 mol. % of proton relative to the FA.

Continuous TH reactions were performed in a plug flow, stainless steel, tubular reactor. The reactor was connected to an HPLC pump in order to regulate the reactant flow and allow operation at elevated pressures. The catalyst was mixed with a diluent material (SiC (particle size of 63-75 μm)), and the catalytic bed placed in between two plugs of quartz wool. The diluted sample was densely packed into a ¼" stainless steel tube (4.1 mm internal diameter), and a frit of 0.5 μm was placed at the reactor exit. The reactor was subsequently immersed in a thermostatted oil bath at the desired reaction temperature. Pressure in the system was controlled by means of a backpressure regulator, and the pressure drop was determined by comparison of the HPLC pump pressure to the outlet pressure measured by a pressure gauge. An overpressure of 5-10 bar was typically employed, depending on reactant flow rate and column length, and this allowed operation above the boiling temperature of the solvent (2-butanol, 98 °C). The reaction feed was identical to that one used for batch reactions. Aliquots of the TH reaction solutions were taken periodically from a sampling valve placed after the reactor. Periodic catalyst regeneration was performed heating the whole reactor in a combustion furnace (Carbolite MTF12/38/400) to 550 °C (10 °C min^{-1}) in air (3 h). All reactants and products during TH were analysed by GC (Agilent 7820, 25m CP-Wax 52 CB column), and quantified against a biphenyl internal standard.

Acknowledgements

CH gratefully appreciates the support of The Royal Society, for provision of a University Research Fellowship (UF140207) and further research grant funding (CH140207). AA-N is indebted to Al-Qadisiya University (Iraq) for the provision of a PhD scholarship. CH also thanks Dr. David Apperley, Dr. Fraser Markwell and Dr. Eric Hughes of the ESPRC UK National Solid-state NMR Service at Durham University for performing the MAS NMR experiments.

References

1 a) J.-P. Lange, *Biofules, Bioprod. Bioref.*, 2007, **1**, 39; b) I. Delidovich, K. Leonhard, R. Palkovits, *Energy Environ. Sci.*, 2014, **7**, 2803; c) T. Ennaert, J. V. Aelst, J. Dijkmans, R. De Clercq, W. Schutyser, M. Dusselier, D. Verboekend, B. F. Sels, *ChemSocRev.* 2016, **45,** 584; d) C. O. Tuck, E. Pérez, I. T. Horváth, R. A. Sheldon, M. Poliakoff, *Science*, 2012, **337**, 695; e) P. Y. Dapsen, C. Mondelli, J. Perez-Ramirez, *ACS Catal.*, 2012, **2**, 1487.

2 I. Sadaba, M. Lopez Granados, A. Riisager, E. Taarning, *Green Chem.* 2015, **17**, 4133.

3 M. J. Climent, A. Corma, S. Iborra, *Green Chem.*, 2014, **16**, 516.

4 a) T. D. Swift, H. Nguyen, Z. Erdman, J. S. Kruger, V. Nikolakis, D. G. Vlachos, *J. Catal.*, 2016, **333**, 149. b) J. M. R. Gallo, D. M. Alonso, M. A. Mellmer, J. H. Yeap, H. C. Wong, J. A. Dumesic, *Top Catal*, 2013, **56**, 1775. c) R. Mariscal, P. Maireles-Torres, M. Ojeda, I. Sádaba, M. L. Granados, *Energy Environ. Sci.*, 2016, **9**, 1144.

5 a) J.-P. Lange, E. van der Heide, J. van Buijtenen, R. Price, *ChemSusChem,* 2012, **5**, 150; b) X. Zhang, K. Wilson, A. F. Lee, *Chem. Rev.* 2016, **116,** 12328; c) H. P. Winoto, B. S. Ahn, J. Jae, *J. Ind. Eng. Chem.*, 2016, **40**, 62.

6 a) A. Corma and M. Renz, *Angev. Chem. Int. Ed*, 2007, **46**, 298; b) M. Koehle and R. F. Lobo*, Catal. Sci. Technol.*,2016, **6**, 3018; c) J. D. Lewis, S. Van der Vyver, A. J. Crisci, W. R. Gunther, V. K. Michaelis, R. G. Griffin, Y. Román-Leshkov, *ChemSusChem*, 2014, **7**, 2255, d) J. Jae, E. Mahmoud, R. F. Lobo, D. G. Vlachos*, ChemCatChem*, 2014, **6**, 508.

7 a) M. Moliner, *Dalton Trans.*, 2014, **43**, 4197; b) P. Y. Dapsen, C. Mondelli, J. Perez-Ramirez; *Chem. Soc. Rev.,* 2015, **44**, 7025; c) H. Y. Luo, J. D. Lewis, Y. Román-Leshkov, *Annu. Rev. Chem. Biomol. Eng.,* 2016, **7**, 663.

8 A. Corma, M. E. Domine, L. Nemeth, S. Valencia, *J. Am. Chem. Soc.* 2002, **124**, 3194.

9 C. Hammond, D. Padovan, A. Al-Nayili, P. P. Wells, E. K. Gibson, N. Dimitratos, *ChemCatChem,* 2015, **7,** 3322.

10 C. Hammond, S. Conrad, I. Hermans, *Angew. Chem. Int. Ed.* 2012**, 51,** 11736.

11 a) P. Hoffmann, J. A. Lobo, *Micropor. Mesopor. Mat.,* 2007, **106**, 122; b) T. Kawai, K. Tsutsumi, *J. Colloid Interface Sci*., 1999, **212**, 310; c) P. Wu, T. Komatsu, T. Yashima, J. Phys. Chem. 1995, **99**, 10923.

12 P. Lanzafame, K. Barbera, S. Perathoner, G. Centi, A. Aloise, M. Migliori, A. Macario, J.B. Nagy, G. Giordano, *J. Catal.* 2015, **330,** 558.

13 D. Padovan, C. Parsons, M. S. Grasina, C. Hammond, *Green Chem.*, 2016,**18**, 50413.

14 L. Liebner, Proc Safety and Env Protection, 2012, **90,** 773

15 C. Hammond, *Green Chem.* 2017, DOI: 10.1039/C7GC001634K; b) G. M. Lari, P. Y. Dapsen, D. Scholz, S. Mitchell, C. Mondelli, J. Perez-Ramirez, *Green Chem.* 2016, **18**, 1249; *c)* J-P. Lange, *Angew. Chem. Int. Ed.*, 2015, **54**, 13186.

16 E. Nikolla, Y. Román-Leshkov, M. Moliner, M. E. Davis, *ACS Catal.*, 2011, **1**, 408.

17 J. Dijkman s, M. Dusselier, D. Gabriels, K. Houthoofd, P. C. M. M. Magusin, S. Huang, Y. Pontikes, M. Trekels, A. Vantomme, L. Giebeler, S. Oswald, B. F. Sels, *ACS Catalysis,* 2015, **5**, 928.

18 a) M. J. Climent, A. Corma, S. Iborra, M. J. Sabater, *ACS Catalysis,* 2014, **4**, 870; b) H. Li, Z. Fang, R. L. Smith Jr., S. Yang, *Prog. Energy Combust. Sci.,* 2016, **55**, 98.

19 a) Lew, C. M.; Rajabbeigi, N.; Tsapatsis, M. Ind. Eng. Chem. Res. 2012, 51, 5364−5366. b) L. Bui, H. Luo, W. R. Gunther, Y. Romań-Leshkov, *Angew. Chem. Int. Ed.* 2013, **52**, 8022.

20 S. Roy, K. Bakhmutsky, E. Mahmoud, R. F. Lobo, R. J. Gorte, *ACS Catal.*, 2013, **3**, 573.

21 T. Kim, R. S. Assary, C. L. Marshall, D. J. Gosztola, L. A. Curtiss, P. C. Stair, *ChemCatChem*, 2011, **3**, 1451; S. Bertarione, F. Bonino, F. Cesano, A Damin, D. Scarano, A. Zecchina, *J. Phys. Chem. B*, 2008, **112**, 2580.

22 A. Omega, M. Vasic, J. A. Van Bokhoven, G. Pirngruber, R. Prins, *Phys. Chem. Chem. Phys.*, 2004, **6**, 447.

23 M. M. Antunes, S. Lima, P. Neves, A. L. Magalhaes, E. Fazio, A. Fernandes, F. Neri, C. M. Silva, S. M. Rocha, M. F. Ribeiro, M. Pillinger, A. Urakawa, A. A. Valenta, *J. Catal.* 2015, **329,** 522.

24 J. W. Harris, M. J. Cordon, J. R. Di Iorio, J. C. Vega-Vila, F. H. Ribeiro, R. Gounder, *Journal Catalysis*, 2016, **335**, 141.

25 R. Bermejo-Deval, M. Orazov, R. Gounder, S. J. Hwang, E. M. Davis, *ACS Catal.,* 2014, **4**, 2288.

26 A. Al-Nayili, K. Yakabi, C. Hammond, *J. Mater. Chem. A.*, 2016, **4**, 1373.